

$$\mathbf{P}_k^a = (\mathbf{I} - \mathbf{K}_k \mathbf{H}_k) \mathbf{P}_{k-1}^a \tag{8}$$

where

$$\mathbf{K}_k = \mathbf{P}_{k-1}^a \mathbf{H}_k^T (\mathbf{H}_k \mathbf{P}_{k-1}^a \mathbf{H}_k^T + \mathbf{R}_k)^{-1} \tag{9}$$

$$\mathbf{H}_k = \left. \frac{\partial \mathbf{M}_k(\mathbf{x})}{\partial \mathbf{x}^T} \right|_{\mathbf{x}=\mathbf{x}_{k-1}^a} \tag{10}$$

In above expression, \mathbf{Y}_k is the field observation in k th iteration, for a static problem, the field observation is a constant during the iteration process; \mathbf{R}_k is the model uncertainty at the k th step; the sensitivity matrix \mathbf{H}_k is defined as the gradient of vector $\mathbf{M}_k(\mathbf{x})$ in the state variable space as defined in Eq. (10). The sensitivity matrix \mathbf{H}_k is recalculated during each iteration (k th iteration) using the assimilated state vector (\mathbf{x}_{k-1}^a) in the ($k-1$)th iteration. As an example, when one pair of observations (namely one maximum ground settlement and one maximum wall deflection) at a given excavation stage are available, the sensitivity matrix \mathbf{H}_k is constructed with components of partial derivatives of vector-value function $\mathbf{M}_k(\mathbf{x})$ with respect to the state variable vector \mathbf{x} at a given iteration (Yang et al. 2011). Specifically for the example, the sensitivity matrix is defined as (Hommels et al. 2005; Yang et al. 2011):

$$\mathbf{H}_k = \left. \frac{\partial \mathbf{M}_k(\mathbf{x})}{\partial \mathbf{x}^T} \right|_{\mathbf{x}=\mathbf{x}_{k-1}^a} = \begin{bmatrix} \frac{\partial M_{kh}(\mathbf{x})}{\partial x_1} & \frac{\partial M_{kh}(\mathbf{x})}{\partial x_2} \\ \frac{\partial h_{kv}(\mathbf{x})}{\partial x_1} & \frac{\partial h_{kv}(\mathbf{x})}{\partial x_2} \end{bmatrix}_{k-1} \tag{11}$$

where x_1 and x_2 is the state variable (referred to herein as soil parameters of s_u / σ'_v and E_t / σ'_v respectively); $M_{kh}(\boldsymbol{\theta})$ and $M_{kv}(\boldsymbol{\theta})$ are the predicted δ_{hm} and δ_{vm} , respectively using the soil parameters x_1 and x_2 at the ($k-1$)th iteration.

Before the iterative process with Kalman filter, the prior estimation of the soil parameters should be obtained based on test data or local experience. The iteration starts from the initial state $k = 0$. The prior mean of soil parameters (state value) is defined as \mathbf{x}_0 and prior model uncertainty matrix is \mathbf{P}_0 . A specific criterion for state value stabilization should be pre-defined before the iteration process. And the convergence is deemed to be reached when the estimated soil parameters in the sequential steps are less than a very small tolerance value, which is defined as:

$$|\mathbf{x}_k^a - \mathbf{x}_{k-1}^a| / \mathbf{x}_k^a < TOL \tag{12}$$

TOL is the pre-defined tolerance value (e.g., 10^{-6} is used herein). When the tolerance criteria for both soil parameters are satisfied, the iteration process is terminated and optimal back analyzed soil parameters are obtained. It should be noted that at the convergence of Kalman filter estimation, as the state vector at two successive iterations converges, the covariance matrix of \mathbf{R}_k at two successive iterations also converges (Yang et al. 2011).

CASE STUDY FOR INVERSE ANALYSIS OF EXCAVATION

A well-documented excavation case history, called the Taipei National Enterprise Center (TNEC) is used to demonstrate the effectiveness of the proposed inverse

analysis procedure based on the extended Kalman filter formulation. TNEC excavation is located in Taipei city with geological profile consisting soft to medium clays. It involves a total of seven stages of excavation to a final depth of 19.7 m. This excavation is supported by a diaphragm wall with 35 m length and 0.9 m thickness. The well-documented field monitoring data in Ou et al. (1998) for this excavation is used for the inverse analysis. The soil parameters normalized undrained shear strength (s_u / σ'_v) and normalized initial tangent modulus (E_i / σ'_v) of the main clay layers are updated based on observations. The prior estimation of s_u / σ'_v at this excavation site is given with a mean of 0.25 and a coefficient of variation of 0.16 and the prior estimation of E_i / σ'_v is given with a mean of 500 and a coefficient of variation of 0.16 (Kung et al. 2003; Juang et al. 2013; Wang et al. 2014).

With the procedure of the extended Kalman filter formulation presented previously, the inverse analysis can be easily performed for updating the predictions for excavation induced ground responses as shown in Figure 1. It should be mentioned that both the field monitoring data about the ground settlement and wall deflection are used in the updating process and the field monitoring data from first two stages are not used in the inverse analysis process and the ground responses at these early are negligible in the inverse analysis process (Juang et al. 2013). From Figure 1, it is observed that the predicted maximum ground settlement and wall deflection for Stage 3 using the prior estimation of soil parameters differs significantly from the field monitored settlement and wall deflection. After Stage 3 excavation is executed, the soil parameters are refined using the inverse analysis procedure with the field monitoring data in Stage 3. With the updated soil parameters in Stage 3, the excavation induced ground responses becomes closer to the field observation data (as shown in “circle” symbols). The inverse analysis continues stage by stage till the final stage. With more field monitoring data used in the inverse analysis process, the predicted ground and wall responses become closer and closer to the field observation data (as shown by the data points approaching to 1:1 match line). It is also observed that, with the updating procedure, the prediction of wall deflection is much better than the prediction of settlement, which is consistent with the observation by other researchers that the ground settlement is more difficult to predict than the wall deflection.

For excavation problems, the main concern for most engineers is the final ground responses induced by excavation, so the predictions at the final stage (at a most critical excavation depth of 19.7 m) are investigated separately as shown in Figure 2 with notation of “x”. The predictions for the final stage made using the updated soil parameters at stages 3, 4, 5, 6, and 7 (reflected by different excavation depths as 4.9 m, 8.6 m, 11.8 m, 15.2 m, and 17.3 m respectively in Figure 2). It is observed that the prediction for the performances at the final stage (e.g., the maximum wall deflection and ground settlement) match better with the field observations as the excavation proceeds. This demonstrated that the soil parameters can be refined with more field monitoring data, which in turn, improve the predictions of ground responses.

The previous inverse analysis is conducted with the field monitoring data for both ground settlement and wall deflection. Then the inverse analysis is repeated by using one type of field observation (ground settlement or wall deflection) alone. The results from three types of inverse analysis scheme are compared in Figure 2.

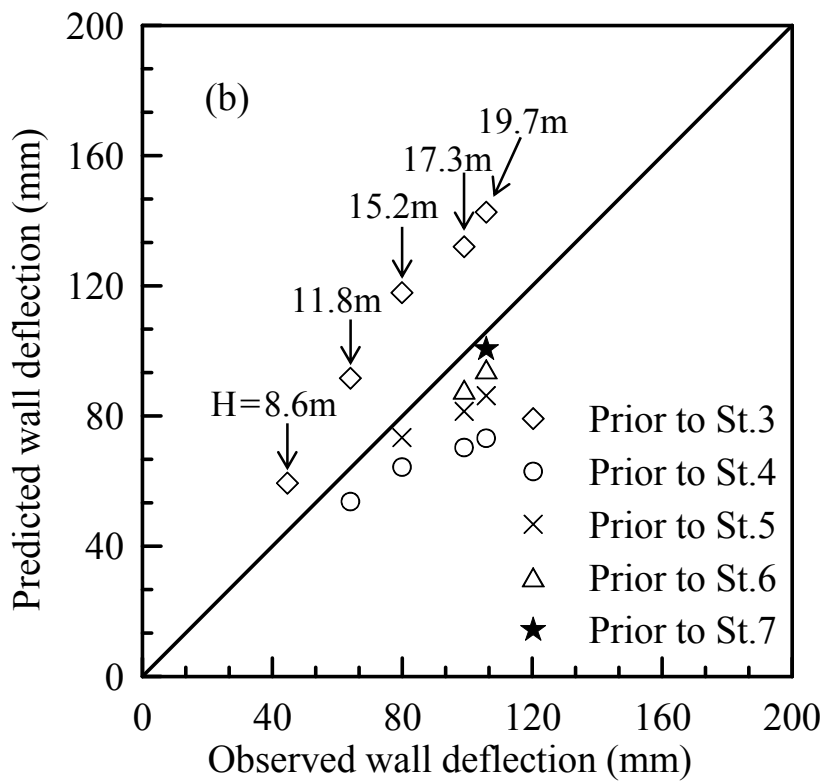
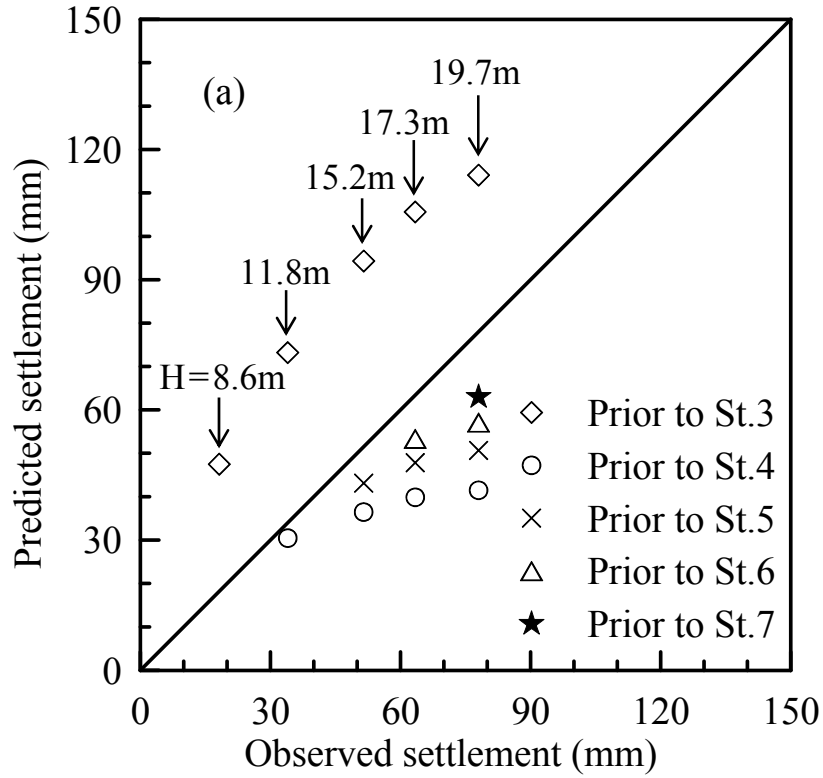


Figure 1. Predictions for maximum ground settlement and wall deflection prior to different stages

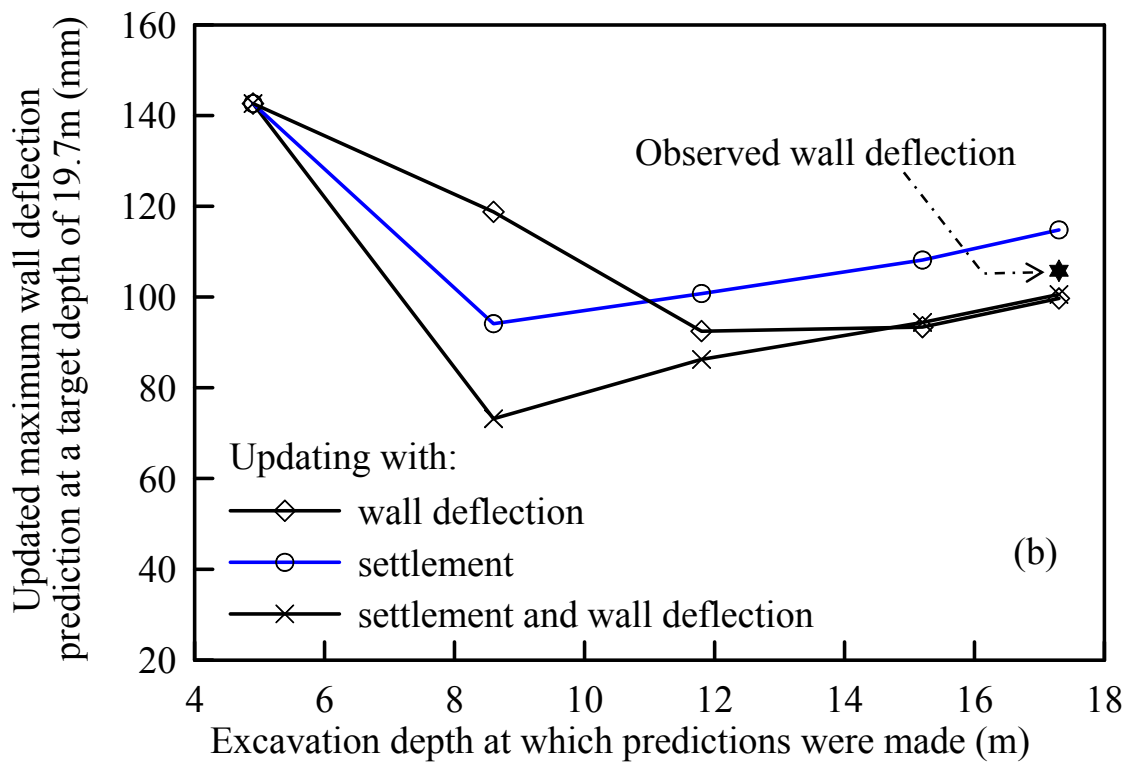
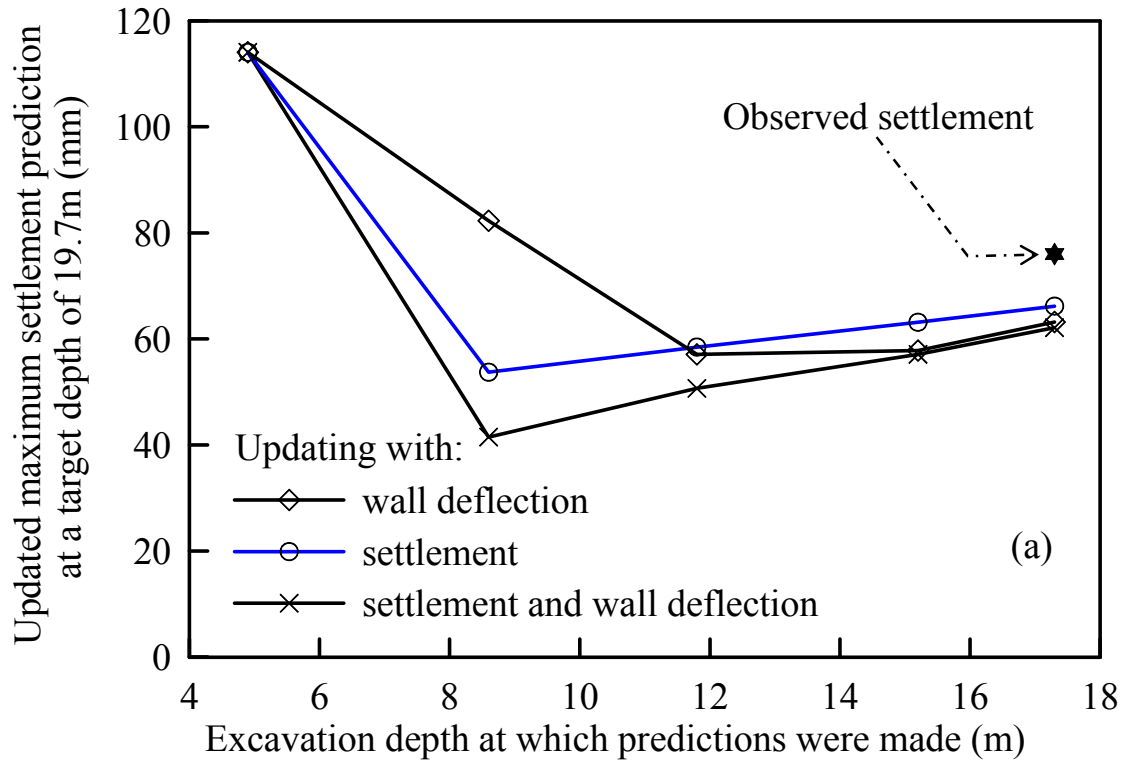


Figure 2. Refined predictions of maximum ground settlement and wall deflection with different updating schemes

As shown in Figure 2, even with one type of field observation, the predicted wall and ground responses at the final excavation stage can be refined as the excavation proceeds. In fact, all three inverse analysis schemes are shown effective in improving the predictions of the excavation-induced wall deflection and ground settlement by incorporating the monitoring data based on the extended Kalman Filter formulation.

The refined soil parameters from the inverse analysis can further be used to predict the damage to adjacent buildings. The procedure developed by Schuster et al. (2009) is employed for assessing damage potential to buildings adjacent to the excavation. The procedure developed Schuster et al. (2009) used a normalization of the principal strain to evaluate the damage potential. The damage potential index (*DPI*) is a function of angular distortion (β) and lateral strain (ϵ_l) that are determined based on soil and structure parameters. The detailed procedure for determining *DPI* is documented in Schuster et al. (2009). The *DPI* value is a *relative* measure for principle strain of the building caused by excavation. *DPI* typically ranges between 0 and 100, and a lower *DPI* value indicates a lower potential for building damage.

For the TNEC excavation, the detailed building properties are documented in Schuster et al. (2009) and Bay No. 4 of Building *D* that is adjacent to TNEC excavation is used as an example for building damage assessment based on Schuster et al. (2009) and Liao (1996). Following similar procedure, the field monitoring data of the earlier stages are used to refine soil parameters based on the inverse analysis procedure, and the refined soil parameters are used to update the damage potential of building adjacent to the excavation in the subsequent stages.

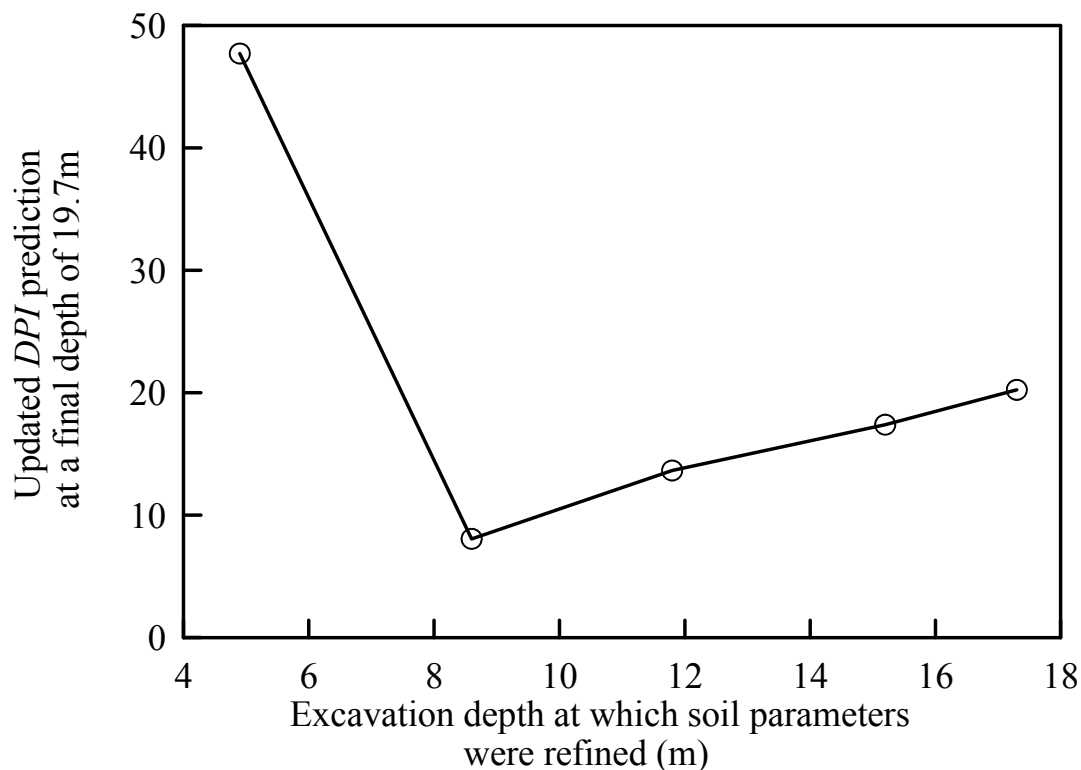


Figure 3. Predicted *DPI* of Building at the final excavation depth with refined soil parameters

Figure 3 illustrates the predictions of the *DPI* at the final excavation depth of 19.7 m using the updated soil parameters prior to different excavation stages (represented as different excavation depths in Figure 3). If the inverse analysis is not performed, the predicted *DPI* prior to Stage 3 (with an excavation depth of 4.9 m) has a very high *DPI* value of about 47.7, for which the building would be classified as “moderate damage” based on the criteria established by Schuster et al. (2009) and would have been inconsistent with the field observation of slight damage. With the refined soil parameters, the predictions of *DPI* are refined step by step with more monitoring data and the prediction prior to the final stage of excavation (with the excavation depth of 17.3 m) yields a *DPI* value of 20.2. Based on Schuster et al. (2009) the building with $DPI = 19$ to 25 would be classified with a “slight damage.” The field investigation found that there are some cracks on the internal walls of Bay No. 4 of Building D after excavation is completed (Liao 1996 and Ou et al. 1998), and was classified as “slight damage” based on the criteria established by Boscardin and Cording (1989). Thus, the refined prediction of *DPI* becomes consistent with field observations through the inverse analysis procedure based on the extended Kalman Filter formulation.

CONCLUSIONS

In this paper, a procedure for inverse analysis of braced excavations based on the extended Kalman Filter formulation is presented and illustrated with a case study of braced excavation in Taipei. In this procedure, the soil parameters are refined using the field monitoring data of the maximum wall deflection and ground settlement. The updating of soil parameters is realized through an extended Kalman Filter formulation combining both the prior estimation and field monitoring data. The updated soil parameters are used to refine and improve the predictions in the subsequent excavation stages. This study demonstrates the effectiveness to learn from the field monitoring data based on the inverse analysis procedure for improving the prediction of excavation induced ground responses, as well as for evaluation of damage potential of adjacent buildings, in a braced excavation in clay.

REFERENCES

- Boscardin, M.D., & Cording, E.J. (1989). "Building response to excavation-induced settlement". *Journal of Geotechnical Engineering*, 115(1), 1-21.
- Calvello, M. & Finno, R.J. (2004), "Selecting parameters to optimize in model calibration by inverse analysis". *Computers and Geotechnics*, 31(5), 411-425.
- Finno, R.J. (2007). "Use of monitoring data to update performance predictions of supported excavations". *Theme lecture in the Proceedings, FMGM, International Symposium on Field Measurements in Geomechanics*, ASCE, Boston, September.
- Finno, R.J., & Calvello, M. (2005). "Supported excavations: the observational method and inverse modeling". *Journal of Geotechnical and Geoenvironmental Engineering* 131(7), 826-836.

- Hashash, Y.M.A., Levasseur, S., Osouli, A., Finno, R. & Malecot, Y. (2010). "Comparison of two inverse analysis techniques for learning deep excavation response". *Computers and Geotechnics*, 37(3), 323-333.
- Hommels, A., Molenkamp, F., Heemink, A.W., & Nguyen, B. (2005). "Inverse analysis of an embankment on soft clay using the Ensemble Kalman Filter". *Proceedings of the Tenth Int. Conf. on Civil, Structural and Env. Eng. Computing*, B.H.V. Topping (Editor), Civil-Comp Press, Stirling, United Kingdom, paper 252.
- Hommels, A., Molenkamp, F., & Heemink, A.W. (2010). "Inverse analysis of a road embankment using the ensemble Kalman filter including heterogeneity of the soft soil". *Proceedings of 1st International Conference on Frontiers in Shallow Subsurface Technology*. Houten, The Netherlands: EAGE.
- Hsiao, E.C.L., Schuster, M., Juang, C.H. & Kung, G.T.C. (2008). "Reliability analysis of excavation-induced ground settlement for building serviceability evaluation". *Journal of Geotechnical and Geoenvironmental Engineering*, 134(10), 1448-1458.
- Juang, C.H., Luo, Z., Atamturktur, S., & Huang, H. (2013). "Bayesian updating of soil parameters for braced excavations using field observations". *Journal of Geotechnical and Geoenvironmental Engineering*, 139(3), 395-406.
- Kung, G.T.C., Juang, C.H., Hsiao, E.C.L., & Hashash, Y.M.A. (2007). "Simplified model for predicting wall deflection and ground surface settlement caused by braced excavation in clays." *Journal of Geotechnical and Geoenvironmental Engineering*, 133(6), 731-747.
- Kung, G.T.C. (2003) "Surface settlement induced by excavation with consideration of small strain behavior of Taipei silty clay". Ph.D. Dissertation, Department of Construction Engineering, *National Taiwan University of Science and Technology*, Taipei, Taiwan.
- Ledesma, A., Gens, A. & Alonso, E.E. (1996). "Parameter and variance estimation in geotechnical back analysis using prior information". *International Journal for Numerical and Analytical Methods in Geomechanics*, 20, 119-141.
- Liao, J.T. (1996). "Performance of a top down deep excavation". Ph.D. Dissertation, Department of Construction Engineering, *National Taiwan University of Science and Technology*, Taipei, Taiwan.
- Ou, C.Y., Liao, J.T., & Lin, H.D. (1998). "Performance of diaphragm wall constructed using top-down method." *Journal of Geotechnical and Geoenvironmental Engineering*, 124(9), 798-808.
- Peck, R. B. (1969). "Advantages and limitations of the observational method in applied soil mechanics". *Géotechnique*, 19(2), 171-187.
- Rechea, C.B., Levasseur, S. & Finno, R.J. (2008). "Inverse analysis techniques for parameter identification in simulation of excavation support systems". *Computers and Geotechnics*, 35(3), 331-345.
- Schuster, M., Kung, G.T.C., Juang, C.H., and Hashash, Y.M.A. (2009). "Simplified model for evaluating damage potential of buildings adjacent to a braced excavation." *Journal of Geotechnical and Geoenvironmental Engineering*, 135(12), 1823-1835.
- Tang, Y.G., & Kung, G.T.C. (2009). "Application of nonlinear optimization technique to back analyses of deep excavation". *Computers and Geotechnics*, 36(1-2), 276-290.

- Tang, Y.G., & Kung, G.T.C. (2010). "Investigating the effect of soil models on deformations caused by braced excavations through an inverse-analysis technique". *Computers and Geotechnics*, 37(6), 769-780.
- Wang, L., Luo, Z., & Juang, C.H. (2013). "Updating uncertain soil parameters by maximum likelihood method for predicting maximum ground and wall movements in braced excavations". *Foundation Engineering in the Face of Uncertainty Honoring Fred H. Kulhawy*, Geotechnical Special Publication 229, pp. 530-541.
- Wang, L., Luo, Z., Xiao, J., & Juang, C.H. (2014). "Probabilistic inverse analysis of excavation-induced wall and ground responses for assessing damage potential of adjacent buildings". *Geotechnical and Geological Engineering*, 32(2), 273-285.
- Yang, C.X., Wu, Y.H., Hon, T., Feng, X.T. (2011). "Application of extended Kalman filter to back analysis of the natural stress state accounting for measuring uncertainties". *International Journal for Numerical and Analytical Methods in Geomechanics*, 35(6), 694-712.
- Zhang, L.L., Zhang, J., Zhang, L.M., Tang, W.H. (2010). "Back analysis of slope failure with Markov chain Monte Carlo simulation". *Computers and Geotechnics*, 37(7-8), 905-912.

Compression Behavior of Foundry Sands

Jie Yin, Ph.D.¹; Ali Soleimanbeigi, Ph.D., P.E., A.M.ASCE²; William J. Likos, Ph.D., M.ASCE³; and Tuncer B. Edil, Ph.D., P.E., D.GE, F.ASCE⁴

¹Research Scholar, Geological Engineering, Univ. of Wisconsin-Madison, Madison, WI 53706; and Associate Professor, Dept. of Civil Engineering, Faculty of Civil Engineering and Mechanics, Jiangsu Univ., Zhenjiang 212013, China. E-mail: jyin34@wisc.edu; yinjie@uj.edu.cn

²Research Scientist, Recycled Materials Resource Center-3rd Generation (RMRC-3G), Univ. of Wisconsin-Madison, Madison, WI 53706. E-mail: soleimanbeig@wisc.edu

³Professor and Chair, Geological Engineering, Univ. of Wisconsin-Madison, Madison, WI 53706. E-mail: likos@wisc.edu

⁴Professor Emeritus and Director, Recycled Materials Resource Center-3rd Generation (RMRC-3G), Univ. of Wisconsin-Madison, Madison, WI 53706. E-mail: tbedil@wisc.edu

Abstract

Beneficial use and recycling of industrial byproducts promotes sustainability in roadway construction. An estimated 15 million tons of waste sands are produced from foundry operations (e.g., casting) in the US annually, out of which less than 28% is recycled and the remainder is landfilled. High-volume structural fill applications such as highway embankments can possibly use the majority of the foundry sands. One of the primary impediments to beneficial reuse of foundry sand in large volumes, however, is uncertainty with respect to its material and engineering properties, including compressibility and volume change. Foundry sand with bentonite binder may exhibit excessive permanent deformations under long-term loading. Compressibility of foundry sands from five different sources in Wisconsin were evaluated in a systematic suite of one-dimensional (1D) and three-dimensional (3D) compression tests. Compacted foundry sands are more compressible than compacted natural sands. Compressibility of foundry sand increases with bentonite fraction and the rate of secondary compression ratio increases with time. Compressibility parameters for foundry were quantified based on bentonite content. Recommended parameters can be used in numerical analyses to estimate creep deformations of embankments constructed with foundry sands at different stress levels, bentonite content, and time since construction.

Keywords: Foundry sand; Compressibility; Highway embankment; Creep.

Introduction

Foundry sand (FSD) is a by-product of the metal casting industry and is a mixture of uniformly graded quartz sand, a small fraction of binding agent (4–16% bentonite clay), a volatile coal additive to prevent casting defects (2–10%), and water (2–5%) (Abichou et al. 2000). Foundries use bentonite as a bonding material, which when added to clean sand, adheres the sand particles together in the mold to form the internal shape and dimension of the casting. Although FSD is reused a number of times by regeneration in the foundry, it ultimately must be replaced and disposed of in order to maintain the required properties for metal casting (Vipulanandan et al. 2000; American Foundry Society 2015). Foundries in the US produce approximately 15 million tons of FSD every year, out of which only about 28% is

beneficially reused, primarily in construction-related applications ([American Foundry Society 2015](#)). The majority of remaining sand is landfilled.

High-volume applications including highway embankment fill or backfill behind retaining structures can possibly use the majority of the FSD ([Lee et al. 2001](#); [Soleimanbeigi and Edil 2015](#)). Beneficial use of FSD in high-volume applications such as embankment fill will promote sustainability in highway construction, reduce consumption of landfill airspace, provide economic alternatives to use of traditional virgin materials, and create new business opportunities ([Benson and Bradshaw 2011](#)). At the current FSD recycling level of 28%, for example, approximately 20,000 tons of CO₂ emissions are prevented and 200 billion BTUs of energy are saved ([EPA 2007](#)). The US EPA Resource Conservation Challenge identifies FSD as a priority material for beneficial use ([Dayton et al. 2010](#)).

One of the primary impediments to beneficial reuse of foundry sand in large-volume construction applications is uncertainty with respect to the material's compressibility ([Javed and Lovell 1994](#)). Because foundry sands contain 0-16% bentonite content ([Goodhue et al. 2001](#)), compression behavior can be significantly different from that of pure sand. Excessive permanent deformations may develop under long-term loading conditions. Permanent deformations (or plastic strain) in embankment construction applications can cause differential settlements, rutting, and cracks in the pavement surface, and creep rupture. Compressibility of structural fill materials, and thus embankment settlement, also affects serviceability of the pavement system. Even if an embankment has adequate overall stability or drainage capacity, the performance of the overlying pavement system can be adversely affected by excessive differential settlement at the road surface, which can reduce the service life by producing ruts and cracks on the pavement.

This paper describes a suite of laboratory experimental tests designed to quantify the compressibility of foundry sands with different bentonite contents for beneficial use as highway embankment fill. Systematic one-dimensional (1D) and three-dimensional (3D) compression tests were conducted for foundry sand samples obtained from five different sources in Wisconsin. Results from the study improve basic understanding of the effects of bentonite content on compressibility characteristics of foundry sand.

Materials

Foundry sand samples were obtained from five different sources in Wisconsin. These included AFK Corporation in Ripon; Arrowcast, Inc. in Shawano; Neenah Foundry in Neenah; Grede Foundries in Milwaukee; and in Browntown. Table 1 summarizes the index and compaction properties of the five FSD samples. Particle size distributions were determined per [ASTM D422](#), and indicated that the FSD samples classified as either clayey sand (SC) or poorly graded sand with silt (SP-SM) according to the Unified Soil Classification System (USCS). Particle size distributions for the five different sands are similar, with the exception of the fines fraction, which ranged from a minimum of 4.1% for the Shawano FSD to a maximum of 14.3% for the Browntown FSD (Table 1). Specific gravity measured in accordance with [ASTM D854](#) was 2.55 on average, which falls within the range from 2.39 to 2.70 for different sources of FSD ([Abichou et al. 2000](#)).

Compaction tests using standard Proctor effort following [ASTM D698](#) were conducted to obtain optimum water contents (w_{opt}) and maximum dry unit weights (γ_{dmax}). Optimum water contents fell within a narrow range between 11.9% and 14.8% for the different foundry sands. The maximum dry unit weights also fell within a narrow range between 17.1 kN/m³ and 18.1 kN/m³. Bentonite contents were determined following a testing procedure proposed by [Abu-Hassanein et al. \(1996\)](#). The bentonite